Solid Freeform Fabrication 2019: Proceedings of the 30th Annual International
Solid Freeform Fabrication Symposium – An Additive Manufacturing Conference
Reviewed Paper

Evaluation of a feed-forward laser control approach for improving consistency in selective laser sintering

T. Phillips*, S. Fish*, J. Beaman*

*Department of Mechanical Engineering, University of Texas at Austin, TX 78712

Abstract

Selective Laser Sintering (SLS) is a popular industrial additive manufacturing technique for creating functional polymer components. One of the biggest limitations today with SLS is its poor mechanical consistency when compared with traditional manufacturing techniques, inhibiting the use of SLS among structurally critical components. Evaluation of the SLS process has revealed that the quality of components is strongly affected by the thermal history during the build process and poor control over this can lead to premature part failure. This paper will discuss a novel technique of improving in-situ thermal control by implementing a feed-forward laser controller that uses dynamic surrogate modelling to predict optimal laser power to achieve desired thermal characteristics. Thermal and destructive testing results will be presented showing that the described laser power controller is capable of decreasing the standard deviations of post sintering temperature by up to 57% and ultimate flexural strength by up to 45%.

Introduction

Selective Laser Sintering (SLS) is a subset of Powder Bed Fusion (PBF) additive manufacturing (AM) that uses a high-powered laser to fuse polymer powder into arbitrary 3D geometries whose features are defined in a 3D CAD file. This is accomplished by depositing a thin layer of polymer powder onto a build surface and scanning a laser across the surface to fuse the material in a shape resembling a 2D cross-section of the final 3D part. Another thin layer of material is spread on top of the previous and the laser now scans the surface according to the next geometric cross-section, fusing this material to the previous layer. Layer-by-layer, the laser fuses the material until the component is completed, after which the un-sintered powder is removed and the 3D component is revealed. While many other AM techniques require supporting structures to ensure the components retain their shape, SLS is capable of creating free-floating components without the need for supports. This enables a user to pack a large amount of components into a single build.

As with most AM techniques, SLS suffers from poor repeatability when compared with traditional manufacturing techniques. Small variations in strength and dimensions exist among additively manufactured components that may limit their usage. Improving component consistency has been the subject of much research and it has been found that laser energy and processing temperature have a large influence on the final component strength [1] [2] [3] [4] [5] [6]. Many of the SLS machines in use unintentionally create thermal gradients on components, leading to the high variability of strength. These thermal gradients can be reduced by implementing a more precise heater system, but eliminating temperature differences across the

powder surface is not possible with these techniques. An alternative approach is to modulate laser energy to account for whatever temperature differences exist on the pre-heated SLS powder. This paper will present a feed-forward approach to modulating laser power in order to reduce post-sintering temperature differences in components. Thermal information is collected in-situ and used in an adaptive surrogate model to predict optimal laser power, which is then sent to the custom laser controller. Testing shows that this technique greatly improves the consistency of components.

SLS Testbed

The experiments presented in this paper were performed on ALM PA650 nylon material using the custom research SLS machine developed at the University of Texas at Austin known as the Laser Additive Manufacturing Pilot System (LAMPS). This system was developed for process control research and exposes all control variables to the user. The laser control technique discussed here makes use of one of LAMPS' thermal cameras, a FLIR A6701. This Mid-Wave Infrared (MWIR) camera is located approximately 1 meter from the build surface at an angle of 28º. It captures 640x512 pixels images at 60 Hz in the 150-300ºC temperature range and has a spatial resolution of approximately 400 μm per pixel. A blackbody is used in-situ for validating temperature values during runtime.

A commercial galvanometer controller is used to control the laser power and position during normal operation of LAMPS. This controller, and every commercial galvanometer controller available at the time of writing, does not allow for intra-vector power changes, meaning obtaining the high level of control over laser power required for overcoming pre-heating thermal gradients is difficult. To overcome this issue, a custom solution was developed that works in conjunction with the commercial controller on LAMPS. This so-called Position-Based Laser Power (PBLP) controller sits between the galvanometer controller and the laser, as seen in Figure 1. The PBLP controller receives the original laser power signal from the galvanometer controller as well as position feedback from the galvanometers and a description of the desired laser power surface from the LAMPS host computer. It uses the original laser power signal from the galvanometer controller as a trigger. When the signal is high, the PBLP controller continuously samples the galvanometer position, solves the laser power surface for that location, and outputs the correct signal to the laser. This allows the PBLP controller to have no knowledge of the laser scan path, yet still actuate the laser at the correct time intervals.

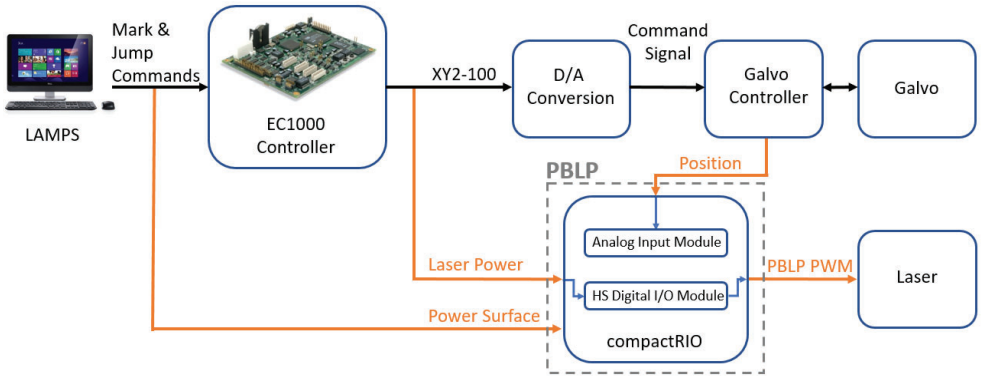

Figure 1: Position-Based Laser Power Controller

Laser Control

A feed-forward laser control technique was developed in order to control the post-sintering temperature of components. Previously, researchers have developed in-situ monitoring techniques and real-time feedback systems for metal additive manufacturing [7] [8] [9] [10]. These systems are successful in homogenizing post-sintering temperatures of metal components, but would be challenging to implement in a polymer SLS system. The difficulty lies in the amount of thermal energy emitted at the processing temperature of polymers, as the amount of energy emitted at the melting temperature of nylon is two orders of magnitude lower than that emitted at the melting temperature of steel. This makes it difficult to find a sensor capable of the 10-20 kHz rate required for real-time control of the laser system [11]. Instead, a feed-forward approach is taken in this paper that allows for the high level of control desired without requiring custom sensors.

In order to properly implement a feed-forward controller for laser power, a model is needed to relate laser energy deposited to temperature increase experienced by the powder. Since the SLS process is highly dynamic, the model should be able to adapt to changes that occur throughout the building process. For this, a dynamic surrogate model was used that relies on in-situ thermal data to model the SLS system. Due to differences in laser power transmission and powder conduction paths, it cannot be assumed that the same laser power produces the same effect on every area of the powder bed. Therefore, the powder bed is discretized into 1mm x 1mm areas, each with their own thermal model.

The MWIR camera records images during each layer and the resulting information can be condensed into two useful images: pre-sintering and post-sintering temperature. The pre-sintering temperature image is simply the MWIR image taken before any lasing has occurred. The post-sintering temperature image is a composite created by taking the maximum value each pixel recorded during lasing. Subtracting the pre-sintering temperature from the post-sintering temperature gives the temperature increase experienced by the powder due to lasing. A perspective transformation and image registration process is performed on each of these images to transform them into the CAD coordinate system. This allows the laser scan files to be used as a mask to extract temperature information from each location that received laser energy, as seen in Figure 2. For each of the 1mm x 1mm areas on the powder bed that received laser energy, the corresponding

thermal model is updated with the new laser power and temperature increase measurement. A weighted linear regression is performed on each model to determine the relationship between delivered laser energy and expected temperature increase for that area. Each new data point is added to its model with a high weight and each time a new measurement is added, all previous measurements have their weight decreased. This produces a forgetting factor that allows the thermal models to deviate from old information that may no longer accurately represent the system [12]. For the experiments discussed here, the forgetting factor was fixed at 0.8, providing a good balance between model stability and system tracking. This process of analyzing the thermal images and updating the thermal models takes place during the powder recoating process after each layer and adds a negligible amount of time to the build.

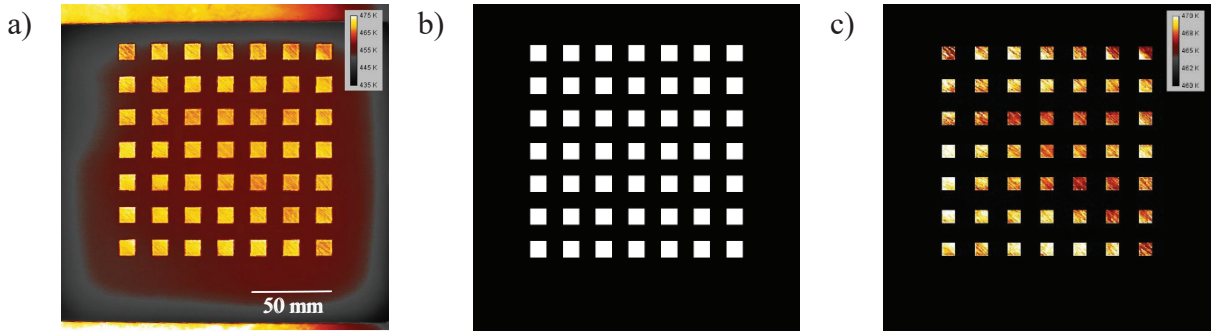

Figure 2: Images depicting (a) a composite post-sintering image after coordinate transformation into machine space, (b) the binary mask created from scan file, and (c) the composite post-sintering image with binary mask applied.

Prior to sintering each new layer, the pre-sintering temperature is measured and the thermal models are consulted to predict the optimal laser power. The laser scan file for the upcoming layer is used to determine which areas are to be lased and, consequently, which thermal models must be queried. For each area that is to be sintered, that area's pre-sintering temperature and desired post-sintering temperature are given to the corresponding thermal model, which predicts the optimal laser power in that area. This is repeated for each of the areas that the laser scan file indicated will be sintered on the upcoming layer. Once the optimal laser power has been predicted for each of these areas, a least-squares regression is performed to fit a parametric surface to the optimal powers and their machine coordinates. An example of such a surface is seen in Figure 3, where the red data are the predicted optimal powers and the blue data is the surface fit to them. The coefficients of this surface are sent to the PBLP controller, which modulates the laser power in real-time to match the desired power surface. A block diagram of this control process can be found in Figure 4.

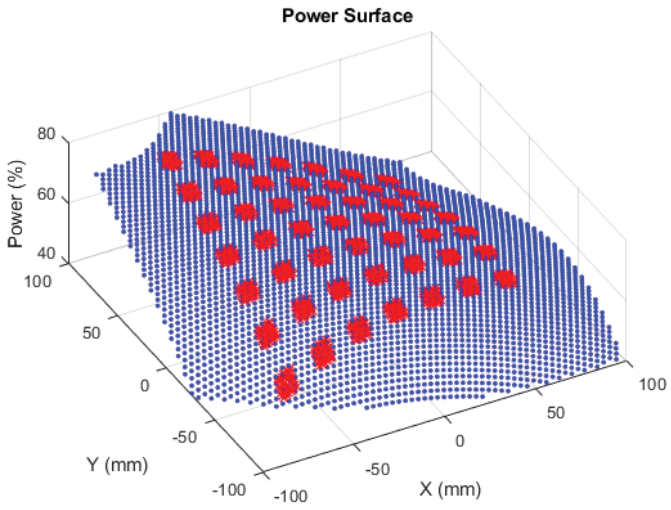

Figure 3: Example power surface

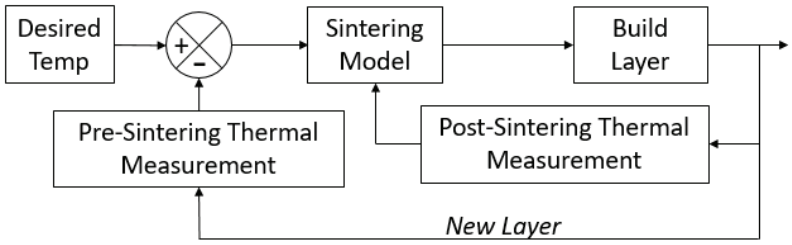

Figure 4: Automated laser control system block diagram

Experiments

The feed-forward laser control technique described above was evaluated by comparing the results it produced with baseline tests that used a pre-determined, fixed laser power regardless of pre-sintering temperature. The first test consisted of 99 flexure bars, 48 of which were built using the automated laser control (ALC) technique. These were built in groups of 10, with ALC and baseline specimens dispersed throughout each build. A total of 110 specimens were built, 10 were determined to have been impacted by a short-feed event during the build process and their data was discarded. Of the remaining 100 components, one failed an interquartile range outlier test for ultimate flexural strength and was also discarded. The specimens had a nominal size of 65mm x 8.5mm x 3.5mm and were tested in accordance with the ASTM D790 testing standard [13]. They were tested in an orientation such that the crosshead motion was normal to the layers, placing the maximum shear plane parallel with the layers.

The next test consisted of two builds of miniature I-beam specimens, one using the ALC technique and the other serving as a baseline for comparison. Each build consisted of 49 identical components whose dimensions are given in Figure 5. These components are not overly complex, but they do have step changes in geometry that stress the laser control system more than the simple geometry of the flexure specimens. Since there is not an appropriate mechanical testing standard

for these components, they were only evaluated for improvement in post-sintering temperature uniformity.

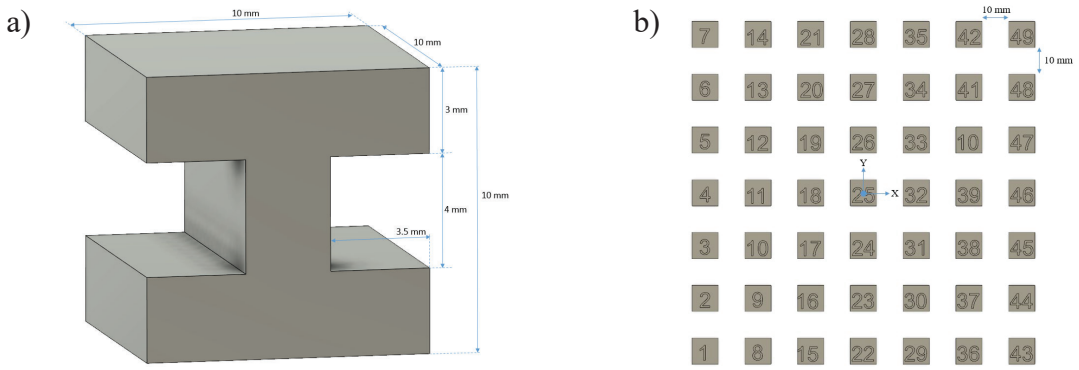

Figure 5: Dimensions of (a) SLS I-beam test part and (b) their arrangement within the build chamber

Results

The temperature results from the flexure specimens showed a large improvement in uniformity of post-sintering temperatures. To quantify the effects of using the automated laser control system, the average post-sintering temperature of each component was measured on each layer. All components built using the ALC system were compared to determine the standard deviation of post-sintering temperatures on each layer. This was repeated for the fixed power components to provide a baseline measurement. The results are given in Figure 6 and show that the baseline standard deviation is approximately 1.4 °C and constant throughout the build. The ALC components start out around the same level of uniformity, but as the build progresses and the surrogate models collect more data, their prediction capabilities improve and the post-sintering temperature standard deviation is reduced to only 0.5 °C. Overall, the ALC system improved temperature uniformity by 57%.

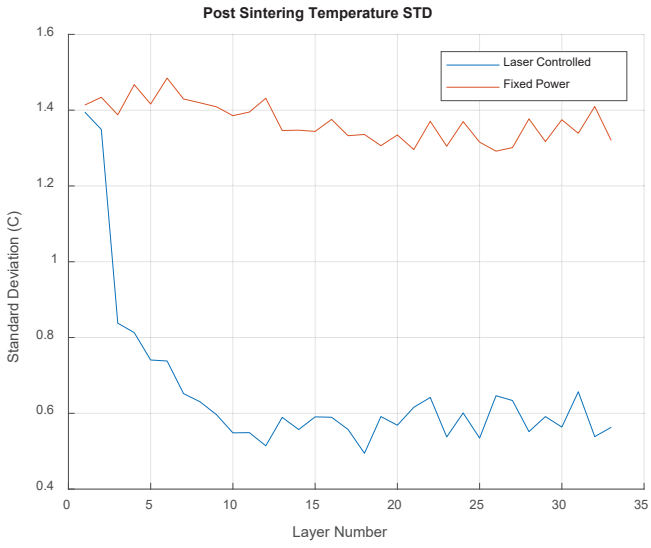

Figure 6: Temperature results from flexure specimens

The flexure specimens were destructively tested and the ultimate flexural strengths for the two groups were binned and fit with a Gaussian distribution. The two distributions were normalized by their own mean so that a direct comparison of standard deviation could be made. These results are presented in Figure 7(a) and show that the standard deviation of ultimate flexural strengths was reduced by 45% when using the automated laser control system. The ultimate flexural strengths are also plotted against their respective post-sintering temperature in Figure 7(b) to highlight how the ALC system drastically reduced the ranges of the strength and post-sintering temperature values, despite having a similar range of pre-sintering temperatures.

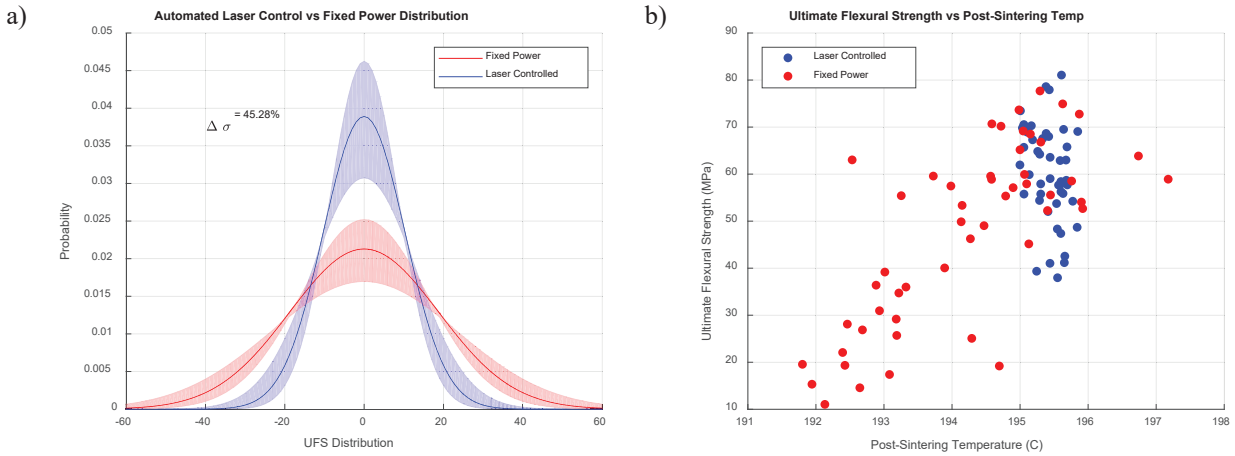

Figure 7: Flexural strength results for Automated Laser Control and baseline components shown (a) as normalized probability distribution and (b) against post-sintering temperature

The I-beam specimens were evaluated for temperature uniformity in the same manner as the flexure specimens. The results, shown in Figure 8, show that the average post-sintering temperature standard deviation was reduced by 45%. The ALC results show an unexplained dip in post-sintering temperature on layer 82 that caused the standard deviation of post-sintering temperatures to be slightly worse than that of the baseline test, though the range was still improved. It is unclear what caused this temperature drop, but the ALC system self-corrected and quickly brought the post-sintering temperature standard deviation back within the desired range. Based on the strength improvements measured by the flexure specimens, it is expected that the strength uniformity of the I-beam specimens was also greatly improved.

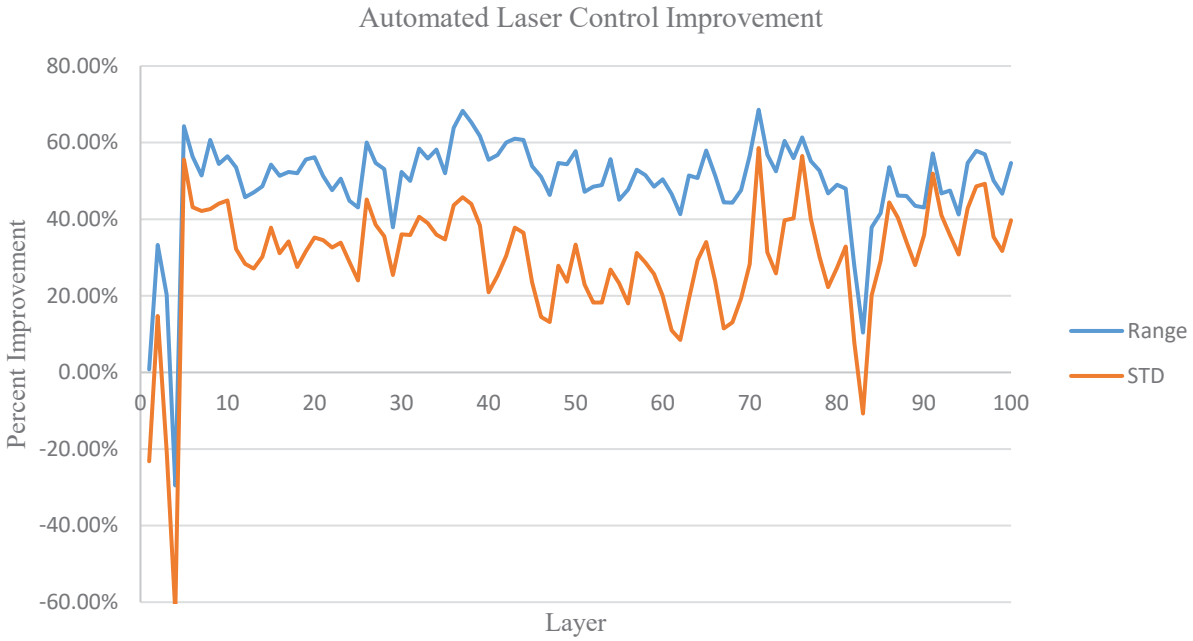

Figure 8: Improvements in I-beam post-sintering temperature uniformity when using Automated Laser Control

Conclusion

This paper covered the implementation of a novel laser control technique for selective laser sintering. The proposed control system was evaluated by comparing the uniformity of components it produced with those produced using a constant laser power. The components showed up to 57% improvement in uniformity of post-sintering temperatures and up to 45% improvement in strength uniformity. Adoption of this system on a commercial machine could lead to more uniform components, a reduced scrap rate, and improved confidence.

There are a few avenues of future work that may increase the impact of this laser control system. First, the desired temperature value used for testing was found empirically through destructive testing of previously built components. A more sophisticated approach might reveal more optimized values that would further improve the strength uniformity improvements. Another area for future work is to test the system on other materials. So far, all testing has taken place on nylon 12, but the control system should be directly applicable to any SLS material. Evaluating the performance of the control system on a variety of materials could improve confidence and utility.

Works Cited

[1] B. Caulfield, P. E. McHugh and S. Lohfeld, "Dependence of mechanical properties of polyamide components on build parameters in the SLS process," *J of Mater Process Technol,* vol. 182, pp. 477-488, 2007.

[2] W. W. Wroe, J. Gladstone, T. Phillips, S. Fish, J. Beaman and A. McElroy, "In-situ thermal image correlation with mechanical properties of nylon-12 in SLS," *Rapid Prototyp J,* vol. 22, no. 5, pp. 794-800, 2016.

[3] S. Negi, S. Dhiman and R. K. Sharma, "Determining the effect of sintering conditions on mechanical properties of laser sintered glass filled polyamide parts using RSM," *Mater,* vol. 68, pp. 205-218, 2015.

[4] I. Gibson and S. Dongping, "Material properties and fabrication parameters in selective laser sintering process," *Rapid Prototyp J,* vol. 3, no. 4, pp. 129-136, 1997.

[5] S. Singh, V. S. Sharma, A. Sachdeva and S. K. Sinha, "Optimization and analysis of mechanical properties for selective laser sintered polyamide parts," *Mater & Manuf Process,* vol. 28, pp. 163-172, 2013.

[6] T. Phillips, S. Fish and J. Beaman, "Development of an automated laser control system for improving temperature uniformity and controlling component strength in selective laser sintering," *Addit Manuf,* vol. 24, pp. 316-322, 2018.

[7] B. Fulcher, *Real-time Pyrometer Feedback and Control in Metal Powder Bed Fusion,* Austin: paper presented to Solid Freeform Fabrication Symposium, 2018.

[8] S. K. Everton, M. Hirsch, P. Stravroulakis, R. K. Leach and A. T. Clare, "Review of in-situ process monitoring and in-situ metrology for metal additive manufacturing," *Mater and Des,* vol. 95, no. 2, pp. 431-445, 2016.

[9] J.-P. Kruth, P. Mercelis, J. V. Vaerenbergh and T. Craeghs, "Feedback control of Selective Laser Melting," in *Proceedings of the 15th International Symposium on Electromachining*, 2007.

[10] M. Grasso and B. M. Colosimo, "Process defects an in situ monitoring methods in metal powder bed fusion: a review," *Measurement Science and Technology,* vol. 28, no. 4, 2017.

[11] T. Craeghs, C. Stijn, E. Yasa and J.-P. Kruth, "Online Quality Control of Selective Laser Melting," in *Solid Freeform Fabr Symp*, Austin, 2011.

[12] D. Rowell, "Introduction to Recursive-Least-Squares (RLS) Adaptive Filters," in *Signal Processing - Continuous and Discrete*, Massachusetts, MIT, 2008.